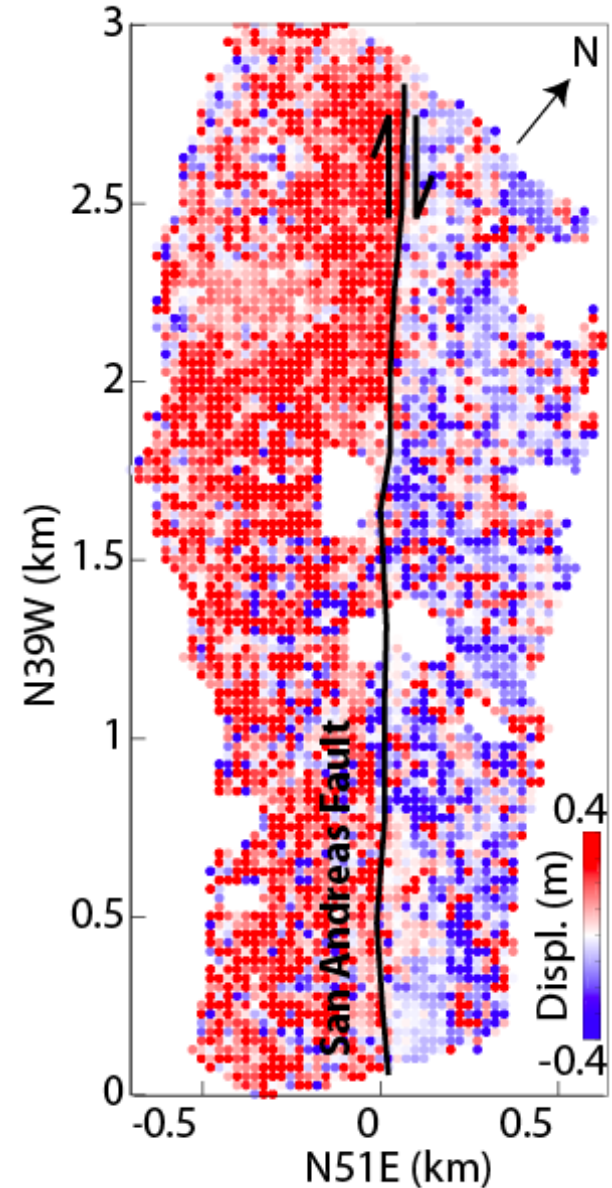


# Quantifying creep rates along the Central San Andreas Fault from repeat high-resolution topography

Chelsea Scott

Coauthors: Ramon Arrowsmith, Stephen DeLong,  
Mike Bunds, Nathan Toke & Manoochehr  
Shirzaei



# Introduction

3D topographic differencing

Fault creep along the Central San Andreas

Two focus areas

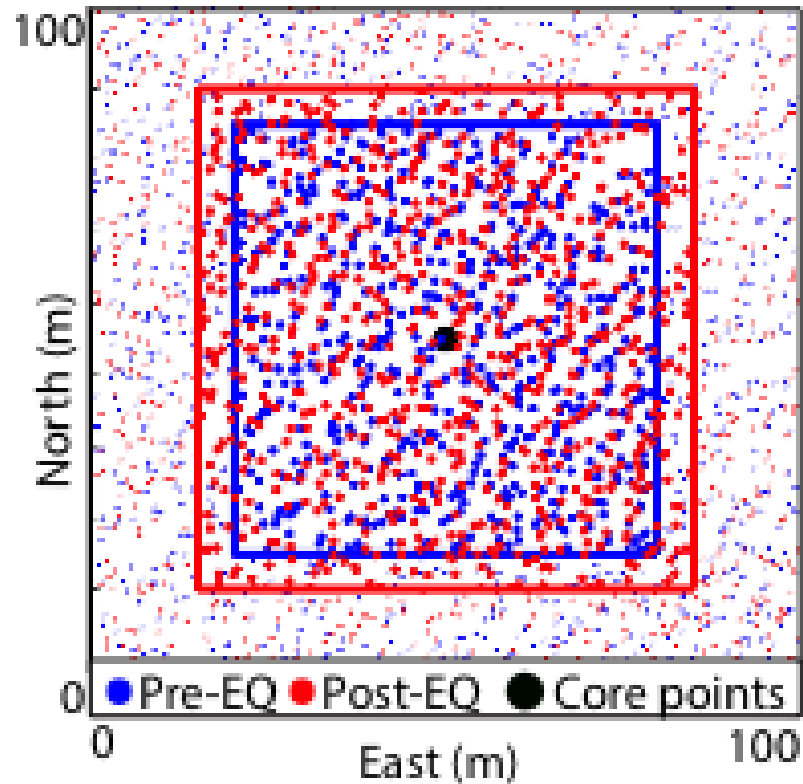
- Mustang Ridge: Deformation along en echelon faults
- Dry Lake Valley: Localized deformation

Persistence through old data to increase time-line:  
1983 Borah Peak earthquake

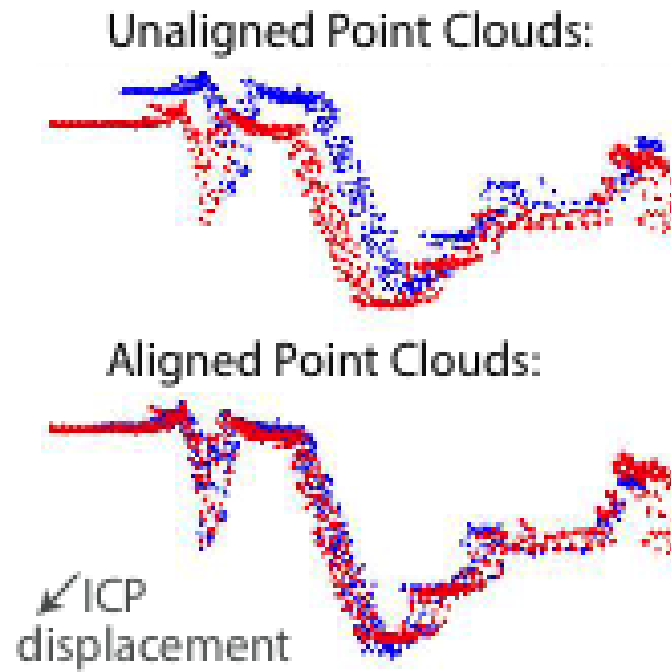


UAV point cloud at Dry  
Lake Valley

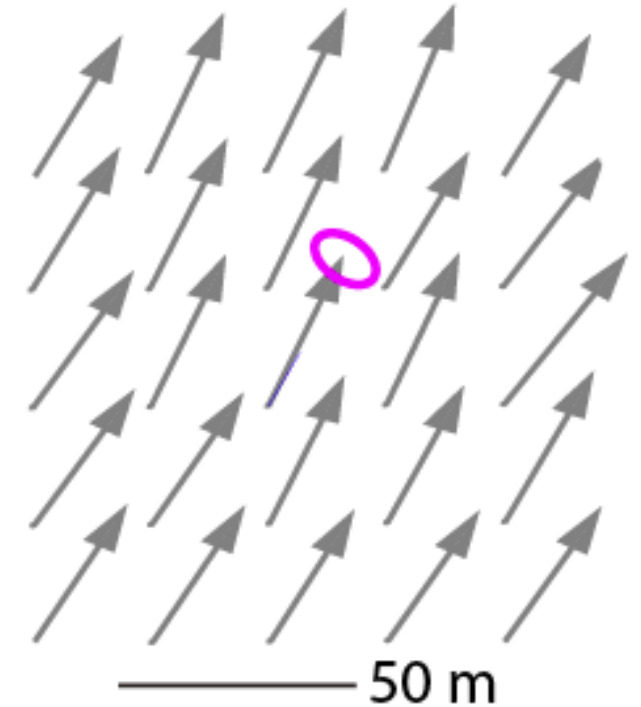
# 3D Topographic Differencing: Iterative Closest Point



Windowed subset of  
lidar topography



3D rigid-body  
deformation

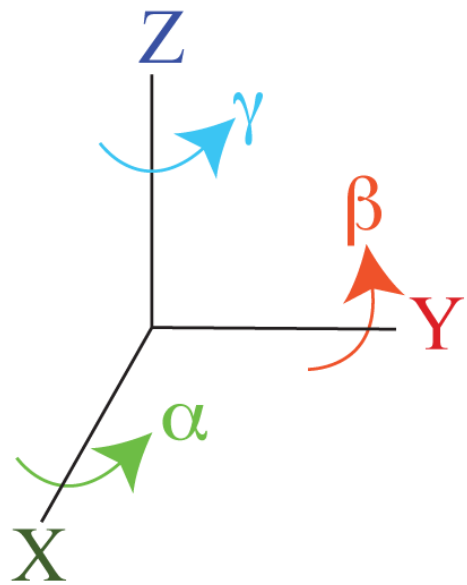


Uncertainty

# 3D coseismic deformation

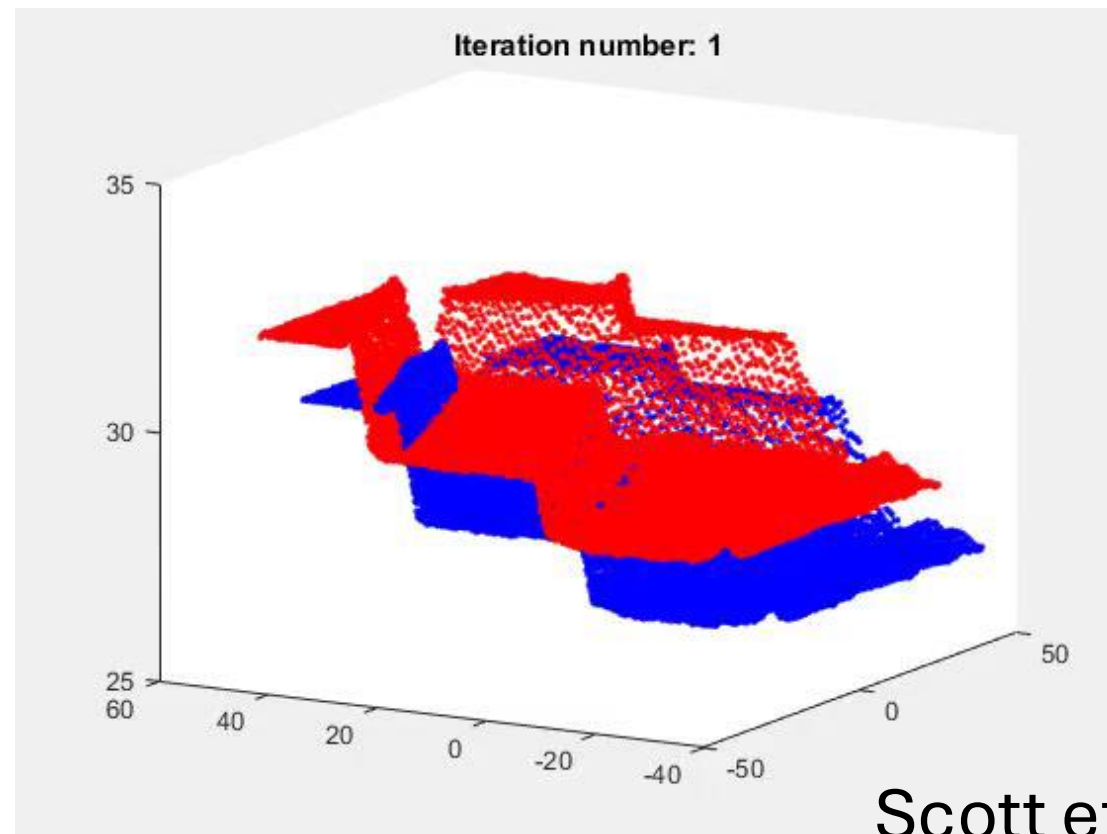
$$\text{Deformed point cloud} = \begin{bmatrix} 1 & -\gamma & \beta \\ \gamma & 1 & -\alpha \\ -\beta & \alpha & 1 \end{bmatrix} \begin{bmatrix} \text{Undeformed} \\ \text{point cloud} \end{bmatrix} + \begin{bmatrix} t_x \\ t_y \\ t_z \end{bmatrix}$$

Rotation      Translation

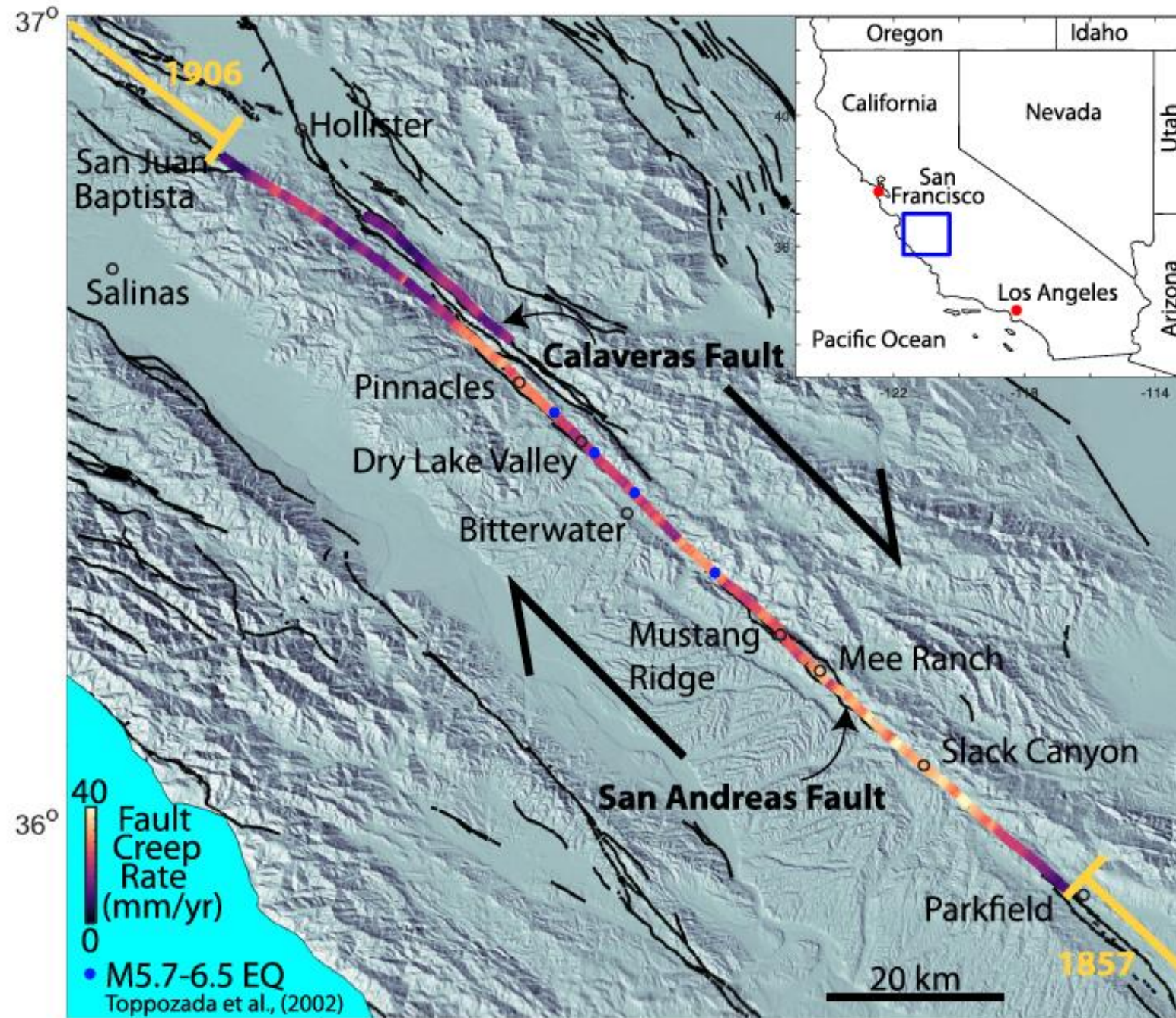


Coordinate system

Rigid body deformation to align pre- and post- earthquake point clouds



# Central California



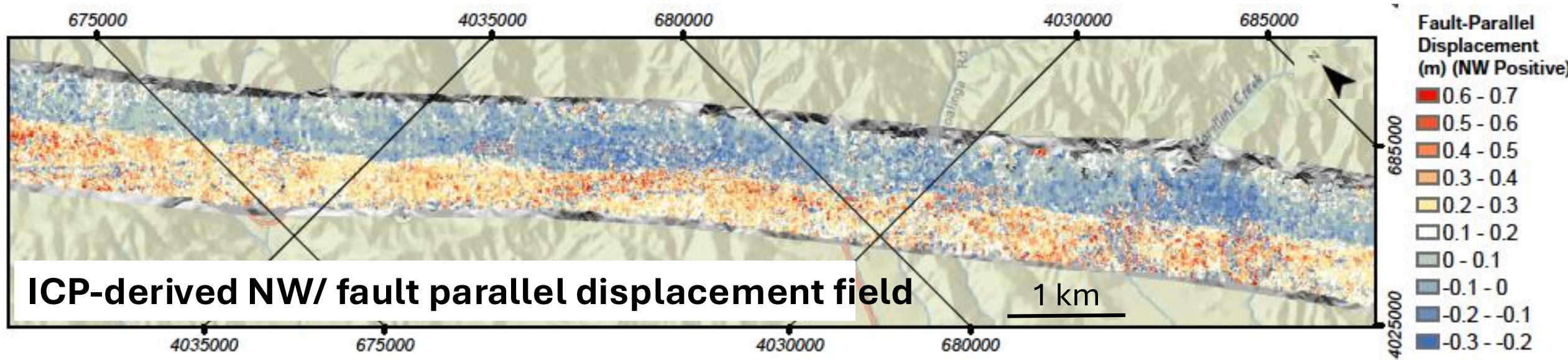
Scott et al. (2020)

Name	Date	pts/m <sup>2</sup>
Lidar		
B4	2005	3
EarthScope	2007	5
Parkfield	2018	11
USGS 3DEP	2018	6
UAV/ drone SfM		
SfM	2019	430

All data available from:



# Displacement field -> Fault creep, creep rate & uncertainty

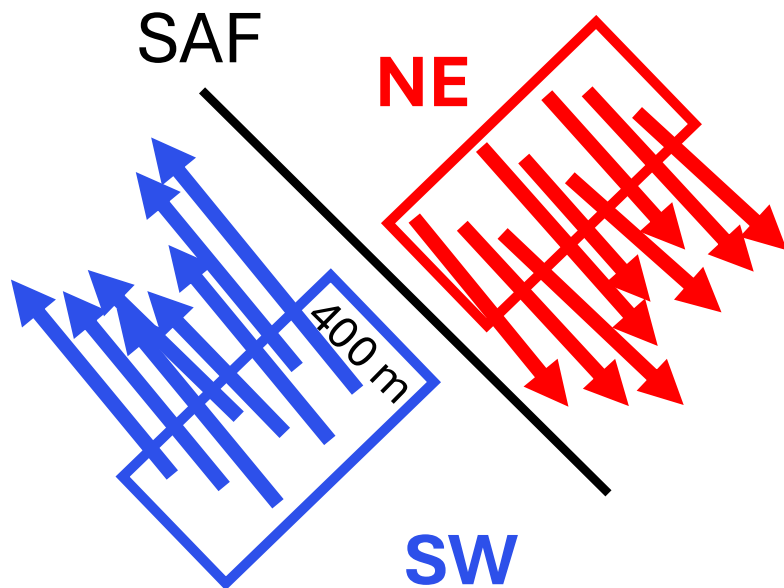


Displacement Discontinuity:

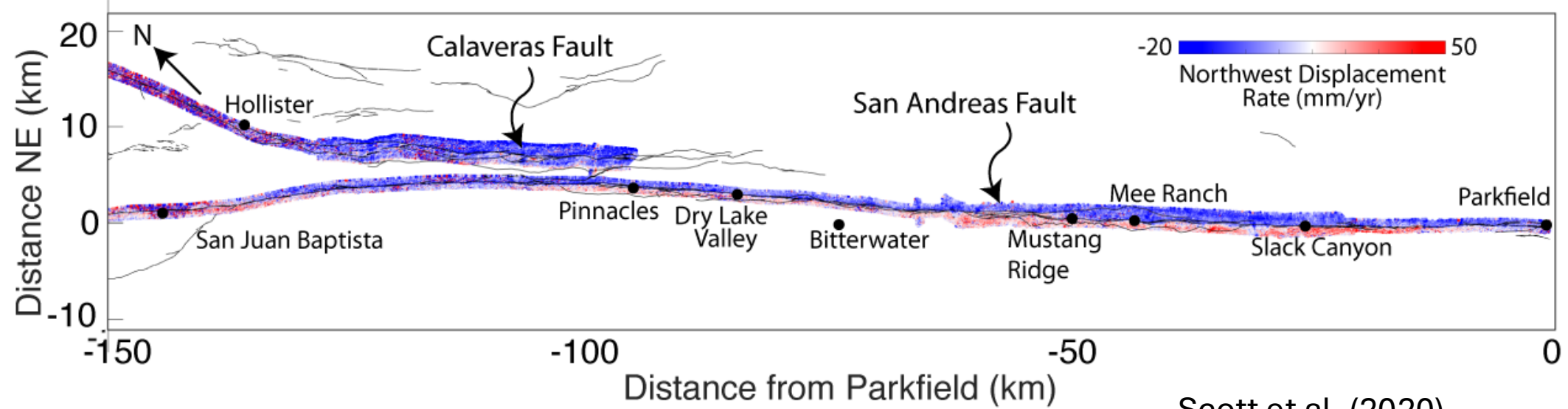
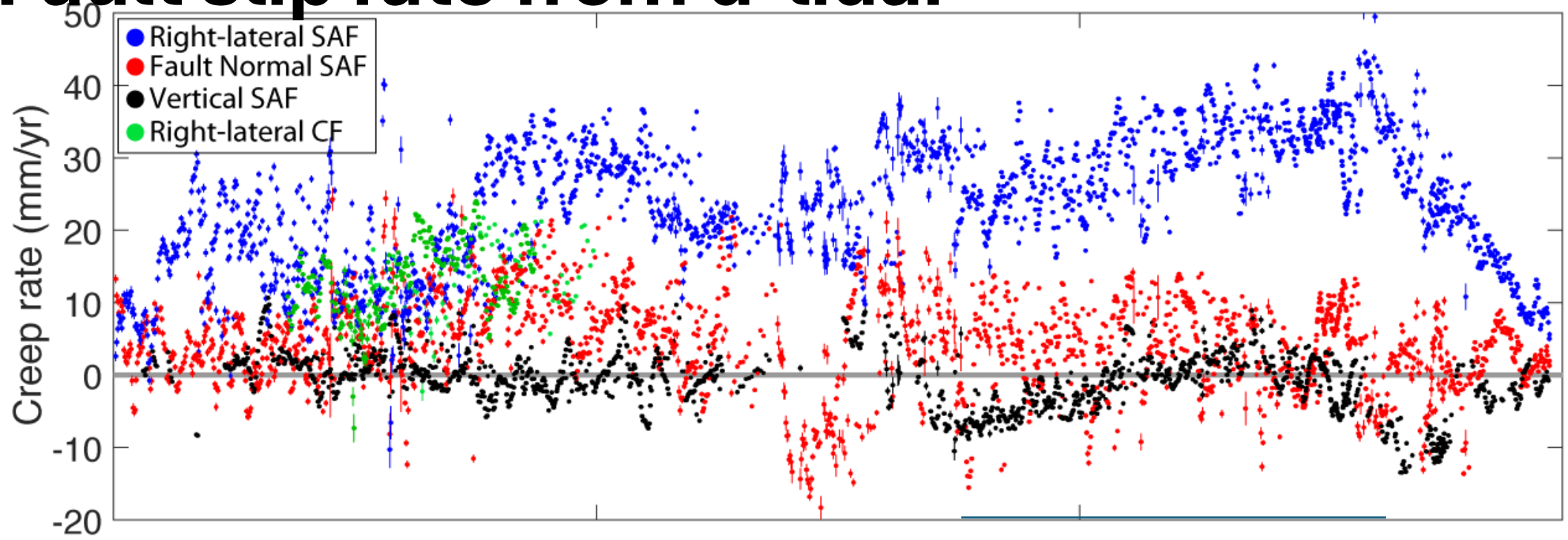
$$\text{Fault Creep} = d_{sw} - d_{ne}$$

$$\text{Fault Creep rate} = \frac{\text{fault creep}}{\text{time}}$$

$$\text{Creep Rate Error} = \sqrt{\Delta d_{sw}^2 + \Delta d_{ne}^2}$$

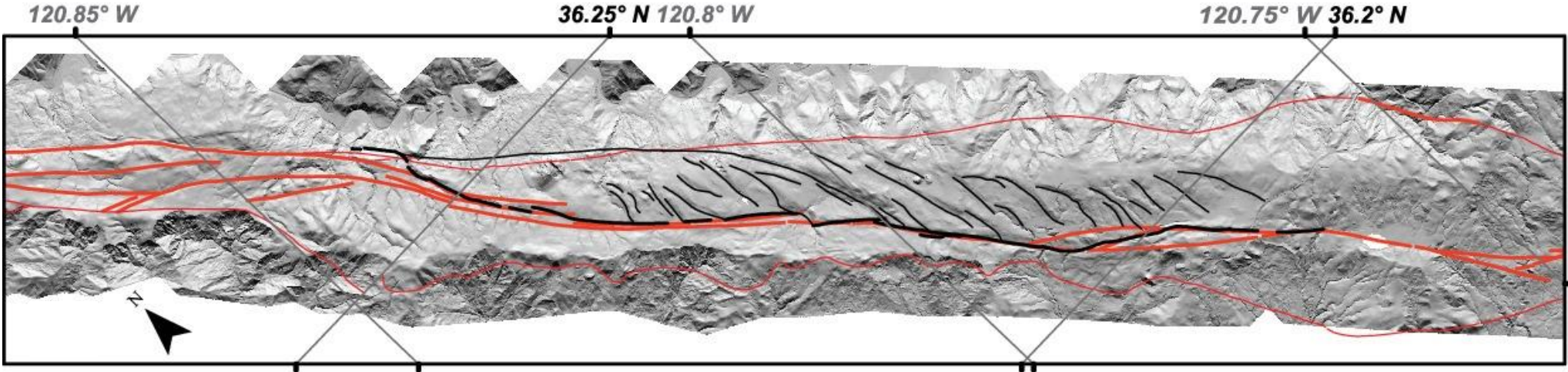


# Fault slip rate from d-lidar



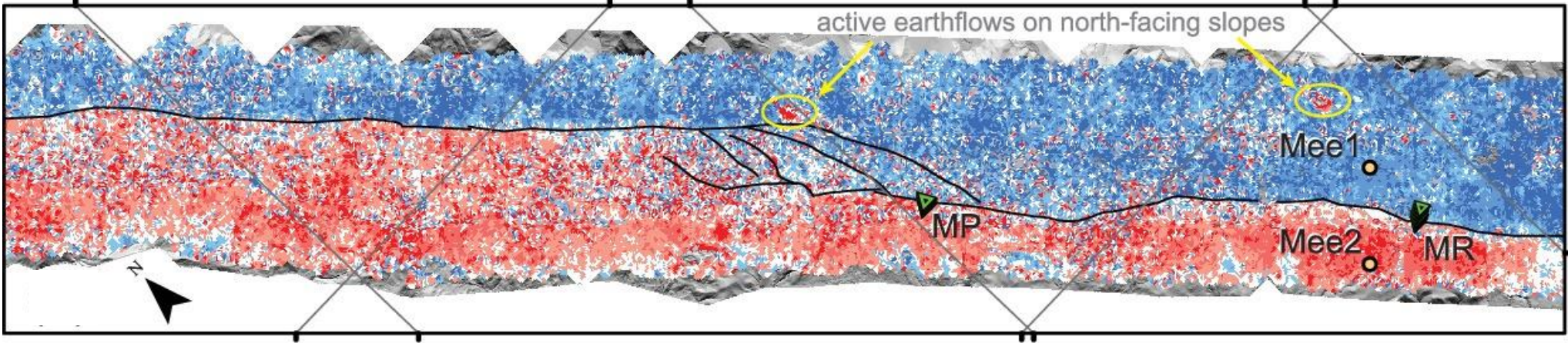
# Mustang Ridge

Right-step through en echelon faults



- USGS/CGS faults**
- Historically Active
  - Quaternary Active
- DeLong et al. 2010 faults**
- Creeping San Andreas
  - Subsidiary fault

Differencing: Similar structural geology but shifted

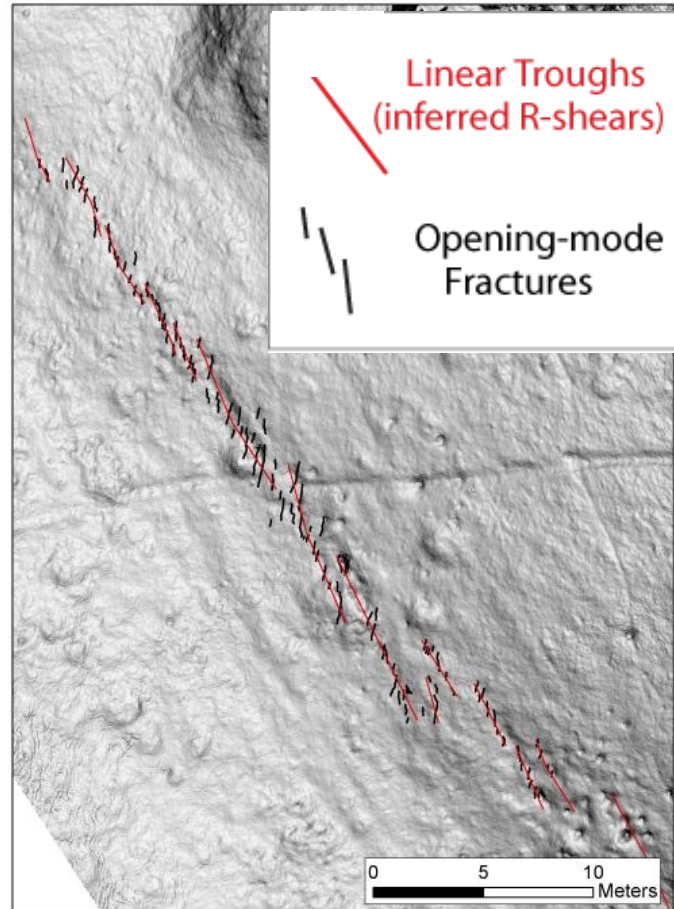
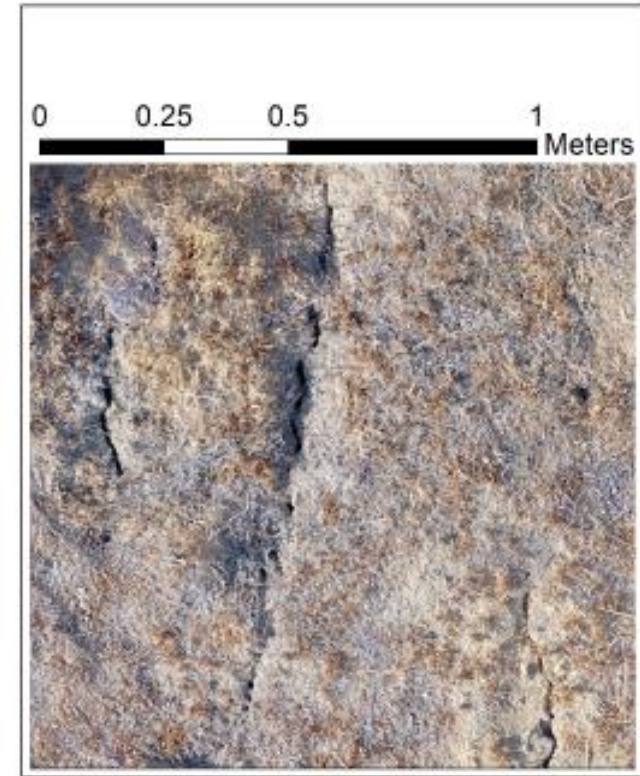


- NW component of ICP analysis (m)**
- 0.3 - -0.2
  - 0.2 - -0.1
  - 0.1 - 0
  - 0 - 0.1
  - 0.1 - 0.2
  - 0.2 - 0.3
  - 0.3 - 0.4
  - 0.4 - 0.5
  - 0.5 - 0.6
  - 0.6 - 0.7
- Creeping San Andreas fault

Distributed deformation

Fault displacement hazard: The active fault may not be most pronounced geomorphically

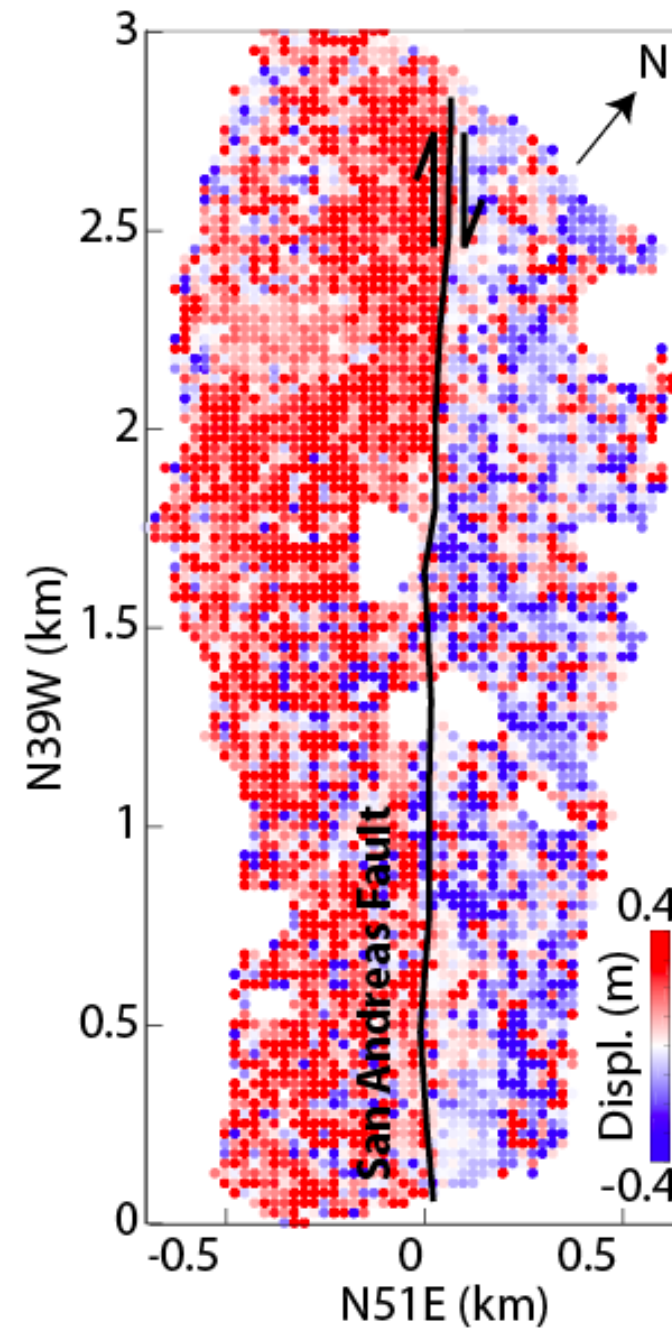
# Dry Lake Valley



Opening mode fractures accommodate  
 $2.2 \pm_{-0.6}^{+0.8}$  cm/yr of fault creep

Scott et al. (2020); Toke and Arrowsmith (2015)

## Lidar- SfM differencing

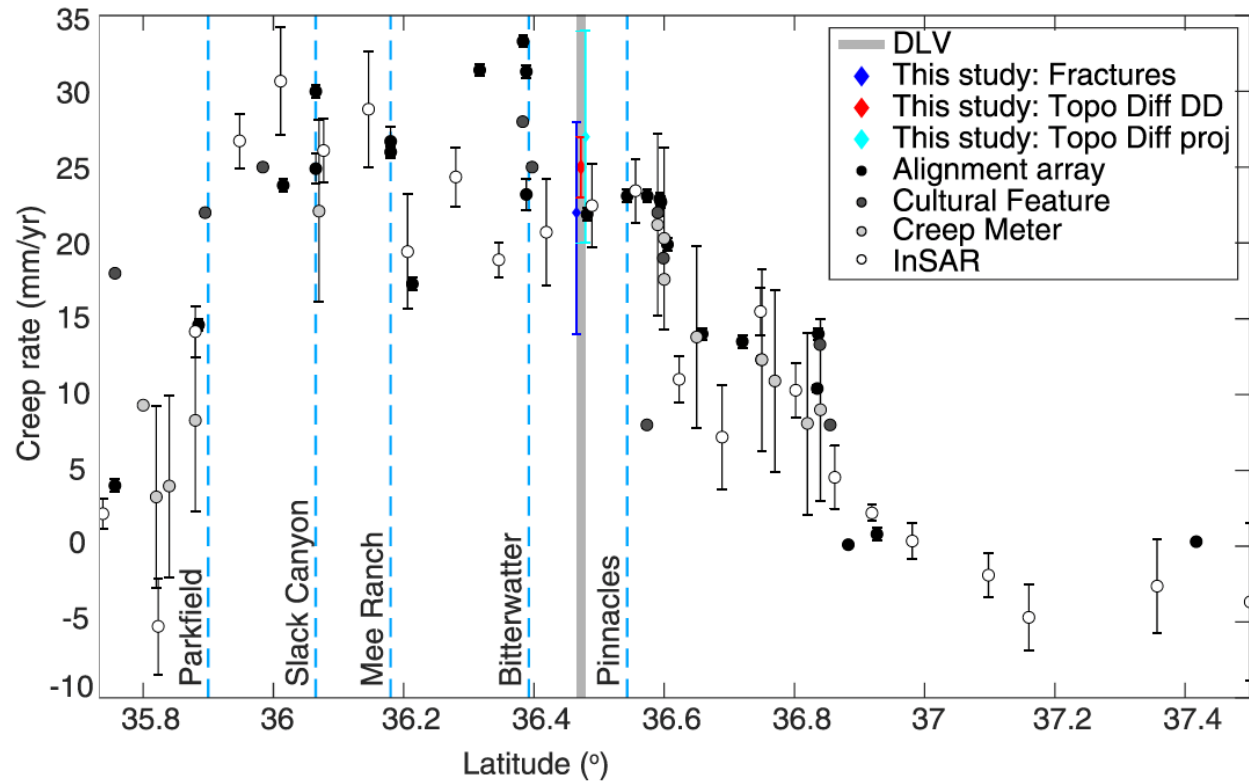


Topographic  
differencing

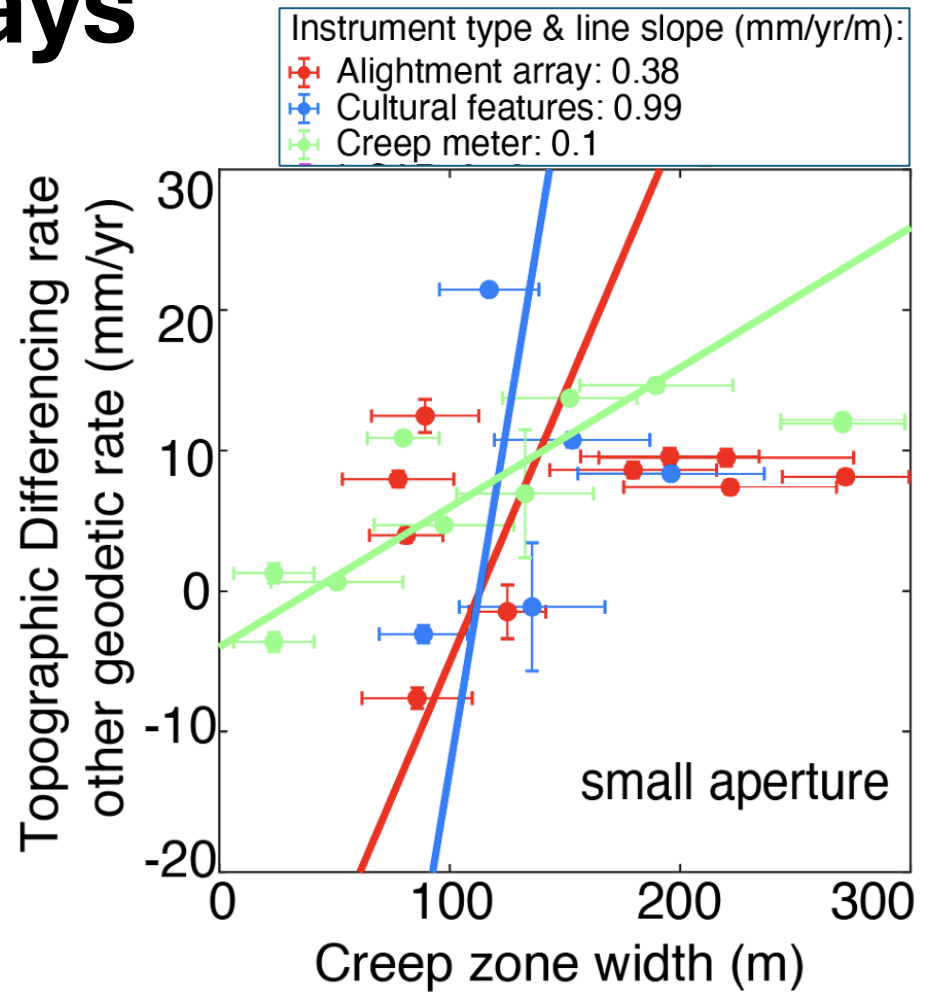
$2.5 \pm 0.2$   
cm/yr

Fractures  
accommodate  
 $90 \pm 30$  % of the  
deformation

# Comparison to alignment arrays



1967- 1974 Alignment array:  $2.19 \pm 0.04$   
cm/yr (Burford & Harsh, 1980)  
Differencing:  $2.5 \pm 0.2$  cm/yr  
Error or creep rate change



Rate differences increase with width  
Deformation is missed by narrow  
aperture

# Publications



## Geophysical Research Letters

RESEARCH LETTER  
10.1029/2020GL090628

### Distribution of Aseismic Deformation Along the Central San Andreas and Calaveras Faults From Differencing Repeat Airborne Lidar



**Key Points:**

- Aseismic fault creep rates are measured over 11–13 years in central California by differencing

Chelsea Phipps Scott<sup>1</sup> , Stephen B. DeLong<sup>2</sup> , and J Ramón Arrowsmith<sup>1</sup> 



## JGR Solid Earth

RESEARCH ARTICLE  
10.1029/2020JB019762

### Creep Along the Central San Andreas Fault From Surface Fractures, Topographic Differencing, and InSAR

**Key Points:**

- We measure tectonic creep along the

Chelsea Scott<sup>1</sup> , Michael Bunds<sup>2</sup> , Manoochehr Shirzaei<sup>3</sup> , and Nathan Toke<sup>2</sup> 



**Caliveras Fault  
Hollister, California**

# 1983 M6.9 Borah Peak, Idaho, earthquake

## Geophysical Research Letters<sup>®</sup>

RESEARCH LETTER

10.1029/2025GL115882

**Key Points:**

- We measured the 1983 M6.9 Borah Peak earthquake's vertical change by differencing 1966 aerial imagery with

**Unveiling Coseismic Deformation From Differenced Legacy Aerial Photography and Modern Lidar Topography: The 1983 M6.9 Borah Peak Earthquake, Idaho, USA**

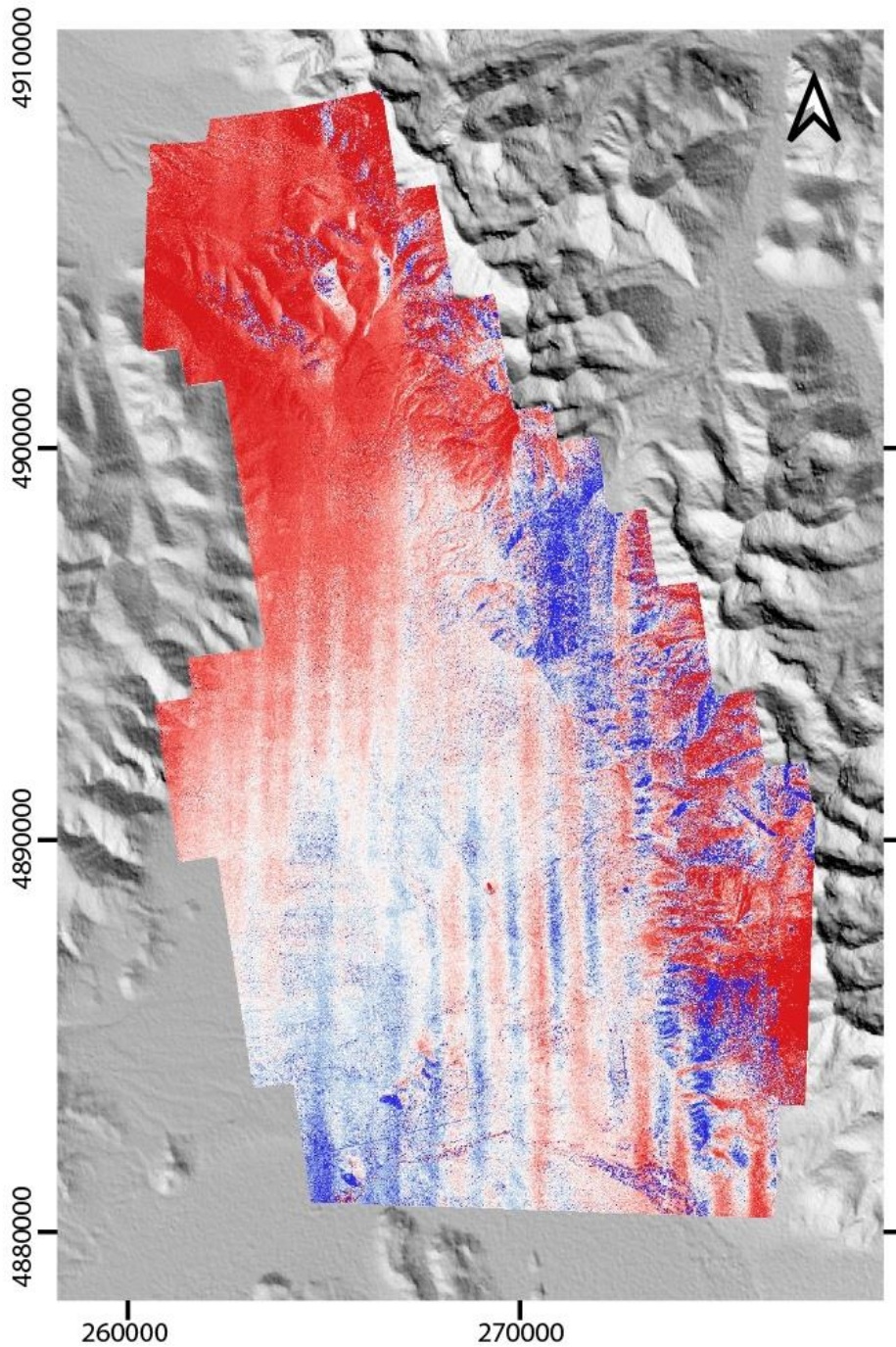
Chelsea P. Scott<sup>1</sup> , Nadine G. Reitman<sup>2</sup> , and Simone Bello<sup>3,4,5</sup> 



Differencing 1996 and 2019- derived topography



# Initial Differencing Results



## Topographic differencing



-6m (down)

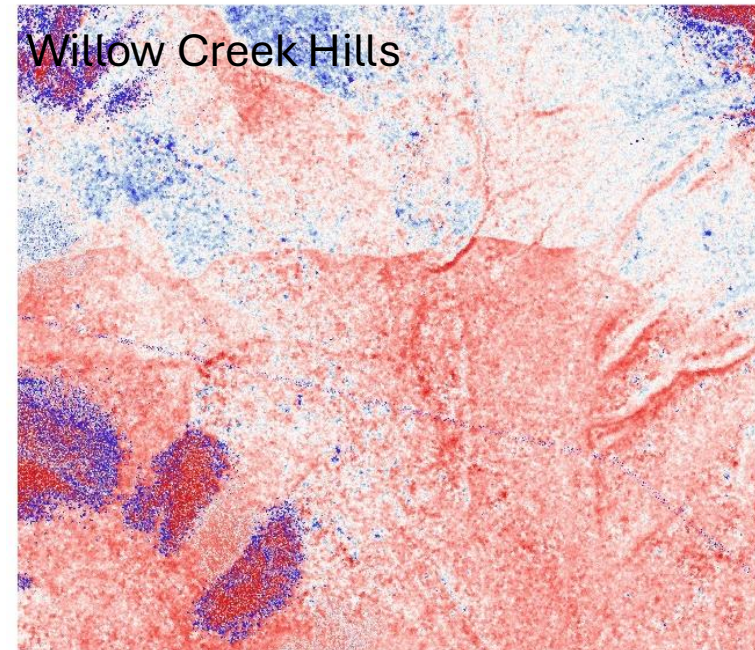
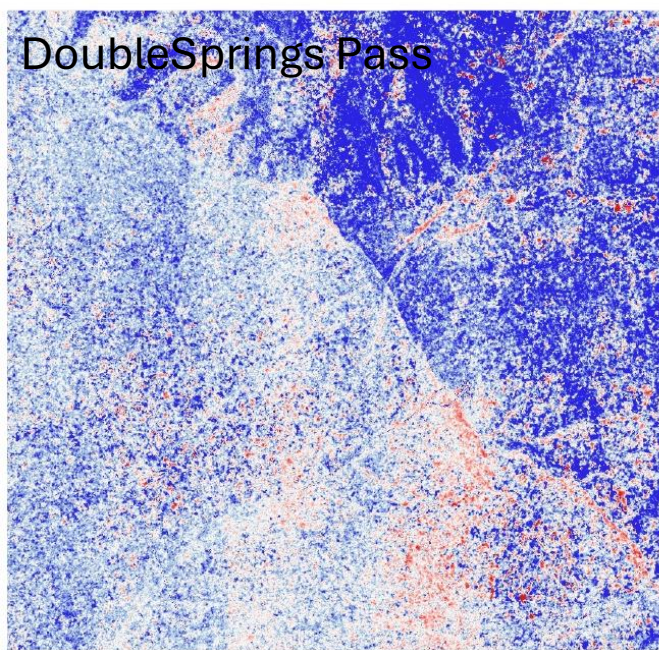
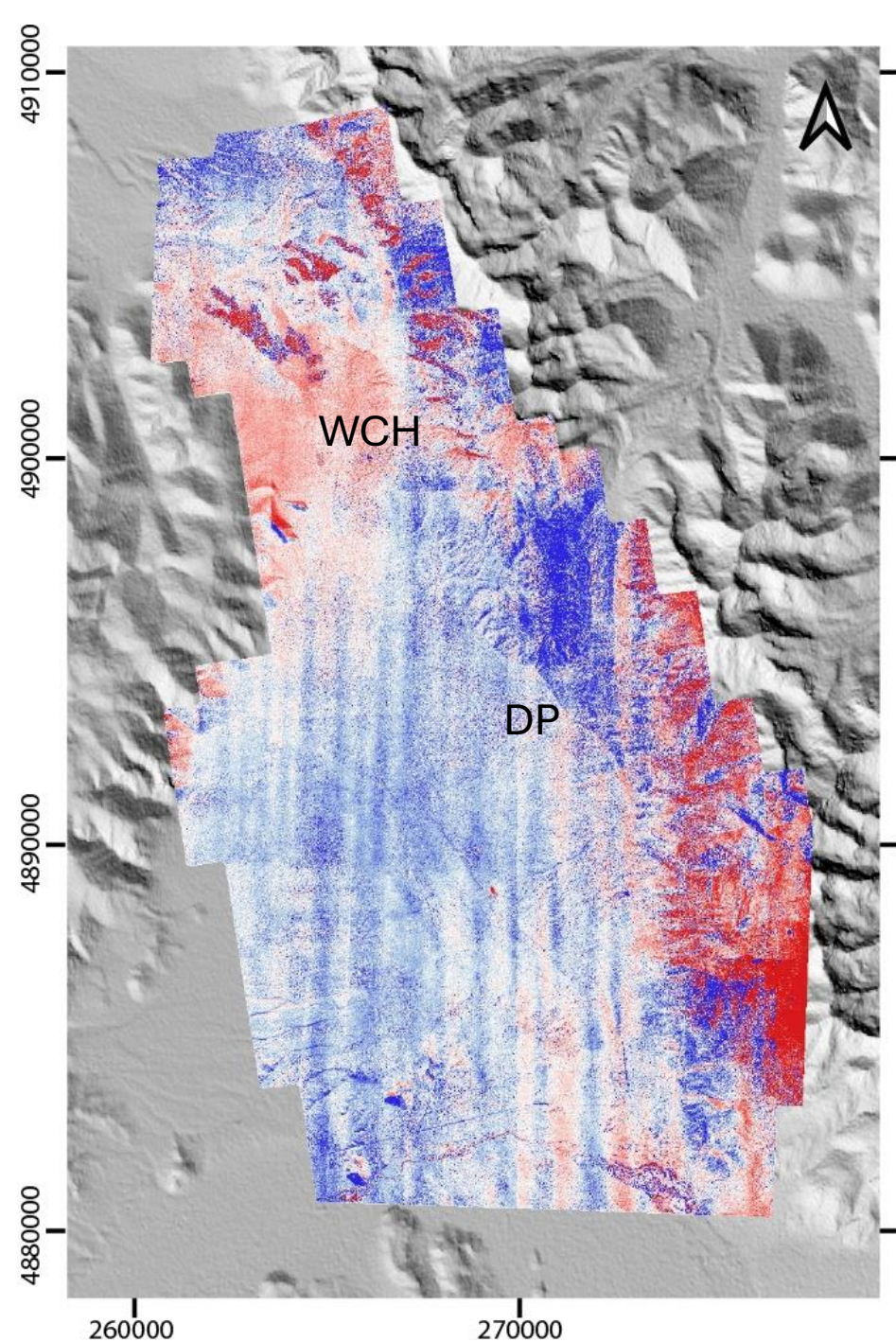


0 m (no change)

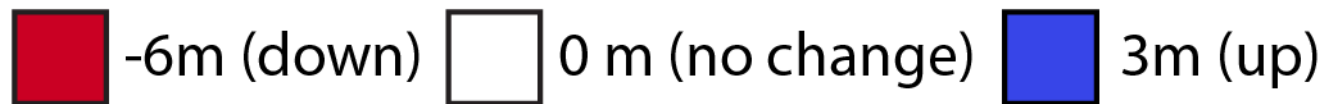


3m (up)

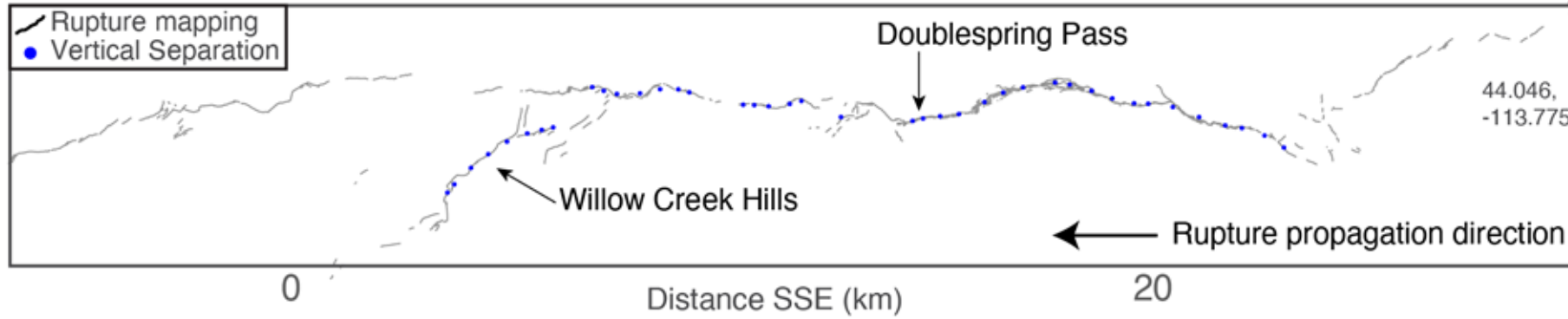
# Improved Differencing Results



## Topographic differencing

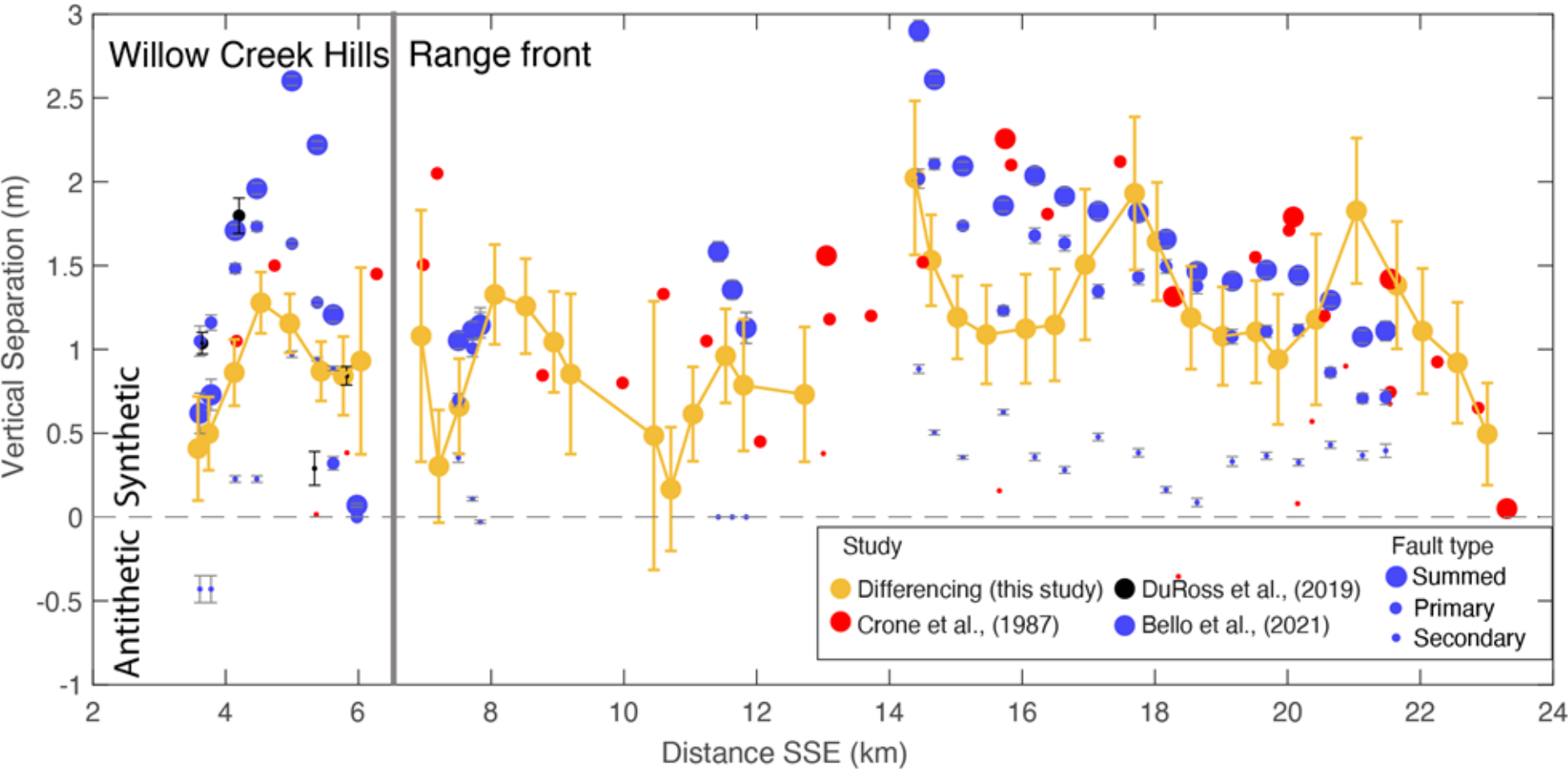


# Vertical Separation: Comparison



Consistency, but other studies are higher

Why? Fault scarp degrades post earthquake.  
Hard to distinguish 1987 from earlier EQ's.  
(Crone et al '87)



Lesson: Value in working with older challenging data to extend timeline backwards

# Conclusions

3D topographic differencing is a powerful technique for measuring fault creep rates and viewing how deformation is accommodated along the faults.

Comparison to alignment arrays:

Similar rates where deformation is localized

Differencing higher for distributed deformation

